Journal of Membrane Science 415–416 (2012) 313–319

Contents lists available at SciVerse ScienceDirect

Journal of Membrane Science

journal homepage: www.elsevier.com/locate/memsci

Fabrication of asymmetric tubular mixed-conducting dense membranes by a combined spin-spraying and co-sintering process

Zhengkun Liu, Guangru Zhang, Xueliang Dong, Wei Jiang, Wanqin Jin*, Nanping Xu

State Key Laboratory of Materials-Oriented Chemical Engineering, College of Chemistry and Chemical engineering, Nanjing University of Technology, 5 Xinmofan Road, Nanjing 210009, PR China

ARTICLE INFO

Article history:
Received 12 December 2011
Received in revised form
12 March 2012
Accepted 6 May 2012
Available online 14 May 2012

Keywords:
Asymmetric tubular membrane
Mixed-conducting membrane
Spin-spraying
Co-sintering
Oxygen separation

ABSTRACT

Mixed-conducting dense ceramic membranes have attracted considerable attention because of their potential application in oxygen separation, oxyfuel combustion and catalytic membrane reaction processes. However, the development of robust mixed-conducting membranes with both high permeability and stability is still a major challenge. In this paper, a crack-free asymmetric tubular membrane made of $SrCo_{0.4}Fe_{0.5}Zr_{0.1}O_{3-\delta}$ perovskite oxide was successfully prepared by a combined spin-spraying and co-sintering method, in which the slurry containing powders was sprayed on a rotating green support tube and followed by sintering process. The issue of the shrinkage mismatch between membrane and support was solved by the optimization of processing parameters, i.e. heating rate, sintering temperature and spraying circles. SEM and nitrogen gas-tight test demonstrated that the surface of membrane was dense, continuous and crack-free, and the thickness of the dense layer was about 20 μm. A high oxygen flux of 7.41×10^{-7} mol cm^{-2} s^{-1} was achieved at 800 °C which was 2.35 times that of symmetric membrane. Long-term oxygen permeation measurement (850 °C, 200 h) showed that the asymmetric membrane was stable under low oxygen partial pressure environment. This work provides a new path for the preparation of asymmetric tubular membrane. This simple and cost-effective fabrication technique can be readily used for mass production.

1. Introduction

Mixed ionic and electronic conducting (MIEC) oxides exhibit both oxygen ionic and electronic conductivities simultaneously at high temperature typically above 700 °C [1]. This feature results oxygen transportation through the MIEC dense membrane in the form of oxygen ions without electrodes and external circuits. Considerable attentions have been attracted on these materials due to their potential application in the oxygen separation, solid oxide fuel cells, membrane reactor and oxyfuel combustion [2–9]. Both high oxygen permeation flux and chemical stability are required for most of these application processes. To improve the stability of MIEC dense membranes, Co-free and/or alkaline earth-free membrane materials are always used [10,11]. Unfortunately, the oxygen permeabilities of these membranes are severely reduced.

Generally, the overall oxygen permeation process through the mixed conducting membrane consists of the following two processes: (i) bulk diffusion through the membrane and (ii) surface reaction on either side of the membrane. When the oxygen permeation is controlled by bulk diffusion, the oxygen permeation flux can be described by the Wagner's equation [12]:

$$J_{O_2} = -\frac{RT}{4^2F^2L}\int_{\ln P''_{O_2}}^{\ln P'_{O_2}} \frac{\sigma_i\sigma_e}{\sigma_i+\sigma_e}\, d\ln P_{O_2} \quad (1)$$

where R is the gas constant; T the temperature; F the Faraday constant; L the membrane thickness; σ_i and σ_e the ionic and electronic conductivities, respectively; P_{O_2} the oxygen partial pressure; P'_{O_2} and P''_{O_2} the high and low oxygen partial pressures in the gas bulk, respectively. From Eq. (1), J_{O_2} is inversely proportional to L. Therefore, the oxygen permeation fluxes can be improved by reducing the thickness of the membrane down to the characteristic thickness L_c. This has triggered the development of asymmetric membranes with oxygen-selective perovskite dense layers on porous supports [13].

Up to date, lots of studies have focused on fabrication of disc-shaped asymmetric membranes via sputtering, dip coating, solution casting, isostatic pressing or other techniques [9,14–20]. Compared with planar discs, tubular structure exhibits obvious advantages, such as easy of scale-up and high-temperature sealing. However, there are only a few works focused on the preparation of asymmetric tubular dense membranes for oxygen or hydrogen separations. Yin et al. [21] fabricated a complete gas-tight thin LSCO/CeO_2 layer on the outer surface of a porous

* Corresponding author. Tel.: +86 25 8317 2266; fax: +86 25 83172292.
E-mail address: wqjin@njut.edu.cn (W. Jin).

0376-7388/$ - see front matter © 2012 Elsevier B.V. All rights reserved.
http://dx.doi.org/10.1016/j.memsci.2012.05.011

CeO_2 tube by slurry coating, and the presence of CeO_2 particles in the membrane layer plays the crucial role in achieving the gas-tight composite membrane. Ito et al. [22] fabricated $SrCo_{0.9}Nb_{0.1}O_{3-\delta}$ the dense membrane with thickness of 50 μm on the porous body also by slurry coating. Kawahara et al. [14] prepared a $La_{0.6}Sr_{0.4}Ti_{0.3}Fe_{0.7}O_3$ thin membrane with 60 μm in thickness on the multichannel structured support by a slip-coating method. Choi et al. [23] described a new technique to fabricate a dense separation layer inside the porous alumina tube by drain casting.

In this work, a new combined spin-spraying and co-sintering process is proposed for the fabrication of asymmetric tubular MIEC dense membrane. The effects of processing parameters on the microstructures and oxygen permeability of the resultant membranes are investigated in detail. By the optimized processing parameters, a dense membrane layer is prepared on the porous tubular substrate with the same composition of $SrCo_{0.4}Fe_{0.5}Zr_{0.1}O_{3-\delta}$ (SCFZ). This work provides a simple and cost-effective technique for the preparation and scaling-up of asymmetric tubular membrane.

2. Experimental

2.1. Synthesis of SCFZ powders

SCFZ powders were synthesized by the solid-state reaction (SSR) method and EDTA–citrate complexation (EC) method. For the SSR method, the required stoichiometric amounts of $SrCO_3$, Co_2O_3, Fe_2O_3 and ZrO_2 were mixed and ball milled for 24 h, followed by calcinations in air at 950 °C for 5 h with heating and cooling rates of 2 °C/min. For the EC method, the required amounts of $Sr(NO_3)_2$, $Co(NO_3)_2$, $Fe(NO_3)_3$ and $Zr(NO_3)_4$ solutions were mixed with EDTA and citric acid (mole ratio of total metal ions to EDTA and to citrate=1:1:2). Ammonia was used to adjust the pH=7. With the evaporation of water at 80 °C the solutions were finally turned to a transparent gel, and then heat-treated in an electrical oven at 250 °C to convert to a solid precursor. The solidified precursors were calcined at 900 °C for 5 h in air.

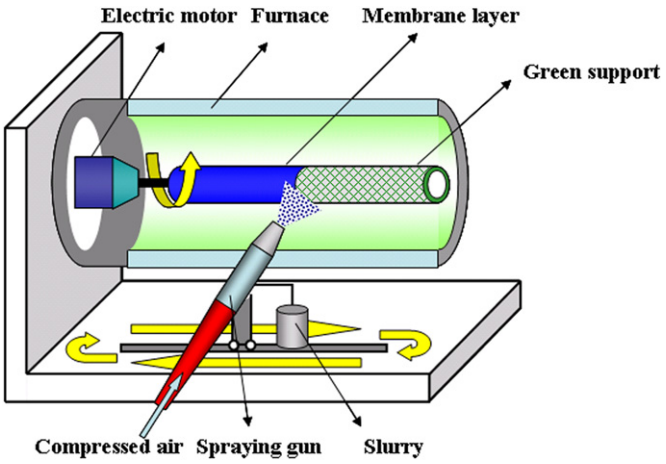

Fig. 1. The schematic diagram of spin spraying method.

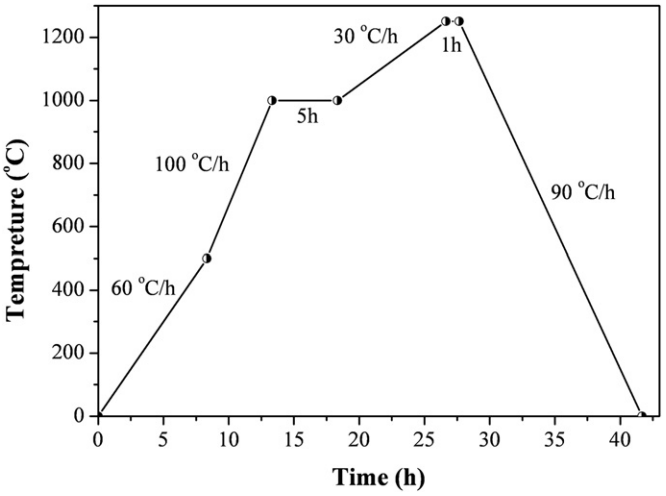

Fig. 2. Heating pattern for sintering the asymmetric tubular membrane.

2.2. Preparation of asymmetric tubular membrane

The plastic extrusion was used to prepare the green thin tubular support. Firstly, the calcined powders were mixed by a minitype vacuum pugmill with several additives, such as inorganic pore former, alcohol (PVA), dextrin, and tung oil to make a formulation (slip) with enough plasticity to be easily formed into the thin tube. Subsequently, the slip was extruded through a die with an orifice diameter and inner diameter of 3.4 mm and 2.2 mm at a high pressure to produce the tube-shaped green support. The calcinated powder was grounded and dispersed in ethanol to obtain a slurry for coating (15–25 wt%). The SCFZ layers were formed on green supports by spin-spraying method. As shown in Fig. 1, the green support tube rotated around central axis at 170 rpm, and the spraying gun moved along horizontal axis at 40 cm/min, then the slurry was sprayed on the support at a rate of 2.5 ml/min. At 100 °C, with the evaporation of ethanol the powders were deposited on the substrate. The resulting tube-shaped asymmetric membrane precursors were sintered at 1250 °C for 1 h. The detailed heating procedure is shown in Fig. 2. For the comparison of oxygen permeability, a SCFZ tubular membrane derived from EC method was prepared by the plastic extrusion. After sintering at 1250 °C for 5 h, the tubular membrane with thickness of 0.5 mm was completely dense and crack-free.

The SCFZ-EC powder was used to fabricate the SCFZ tubular membrane. The membrane was completely dense after sintering at 1250 °C for 5 h. The thickness of SCFZ tubular membrane is 0.5 mm.

2.3. Characterization

The particle size of the SCFZ powders was analyzed by a laser granulometer (MALVERN, model ZETASIZER 3000HSA). The crystal phase of the synthesized SCFZ powders were determined by X-ray diffraction (XRD) with Cu Kα radiation (Bruker, model D8 Advance). The diffraction patterns were collected at room temperature by step scanning at an increment of 0.05° in the range of $20° \le 2\theta \le 80°$. The sintering behavior of green tubular support and membrane layer was measured in the stagnant air with the heating rate of 2 °C min^{-1} using the apparatus of dilatometer (Netzsch, model DIL 402C). The morphology of the asymmetric tubular membrane was examined by environmental scanning electron microscopy (ESEM) (FEI, model QUANTA-200). A gas-tight test was conducted on the sintered asymmetric membrane using nitrogen at room temperature. The porosity of support was evaluated by the Archimedes method.

2.4. Oxygen permeation measurement

Oxygen permeation was conducted using the dense asymmetric tubular membranes without any defects, which were

checked by home-made gas tight measurements before assembly. The membrane module used for oxygen permeation measurements is illustrated in Fig. 3. An asymmetric tubular membrane with the length of 5.4 mm was sealed with two dense Al_2O_3 ceramic tubes (i.d.=2.5 mm, o.d.=4.5 mm) at both the ends of the membrane. A quartz tube surrounding the two alumina tubes formed the shell side of the cell. The shell side of the tubular membrane was exposed to air, whereas the tube side was exposed to helium. The inlet gas flow rates were controlled by mass flow controllers, which were calibrated by a bubble flowmeter. Both sides of the membrane were maintained at an atmospheric pressure. A programmable temperature controller (Model AI-708PA) monitored the temperature around the membrane. The effluent streams were analyzed by an on-line gas chromatograph (Model Shimadzu GC-8A), which equipped with a 2 m 5 Å molecular sieve operated at 50 °C with helium as the carrier gas.

The leakage of oxygen through the seal was usually less than 5% of the total oxygen flux. Assuming that leakage of nitrogen and oxygen through pores or cracks in accordance with Knudsen diffusion, the fluxes of leaked N_2 and O_2 are related by $J_{N_2}^{Leak} : J_{O_2}^{Leak} = \sqrt{32/28} \times 0.79/0.21 = 4.02$. Thus, the oxygen permeation rate was then calculated as follows: J_{O_2} (mL/min/cm^2) $= [C_O - C_N/4.02] \times Q/S$, where C_O and C_N are the concentration of oxygen and nitrogen calculated from the GC measurements, Q is the flow rate of the sweep stream, and S is the membrane area calculated according to $S = (\pi w(d_1 - d_2)/\ln(d_1/d_2))$, where w, d_1 and d_2 are length, outside diameter and inside diameter of the thin tube, respectively.

3. Results and discussion

3.1. The properties of the ceramic powder

To avoid the thermal expansion mismatch and no reactions between the support and the dense membrane layer, the same materials were used for both the porous substrate and membrane [24]. For the preparation of asymmetric membranes, control of the morphology of the precursor particles is very important. Usually, sintering of small particles with a narrow size distribution would easily produce a dense layer due to their good packing density. Powders synthesized by different methods may result in different particle sizes and sintering activities. The average particle sizes of SCFZ-SSR and SCFZ-EC were 9.01 and 4.33 μm, respectively, which were analyzed by a laser granulometer. Therefore, we used the SCFZ-SSR and SCFZ-EC powders as raw materials of support and membrane, respectively. Fig. 4 shows the X-ray diffraction patterns of SCFZ-SSR and SCFZ-EC powders. All the samples showed a cubic perovskite structure with a trace of the $SrZrO_3$ phase.

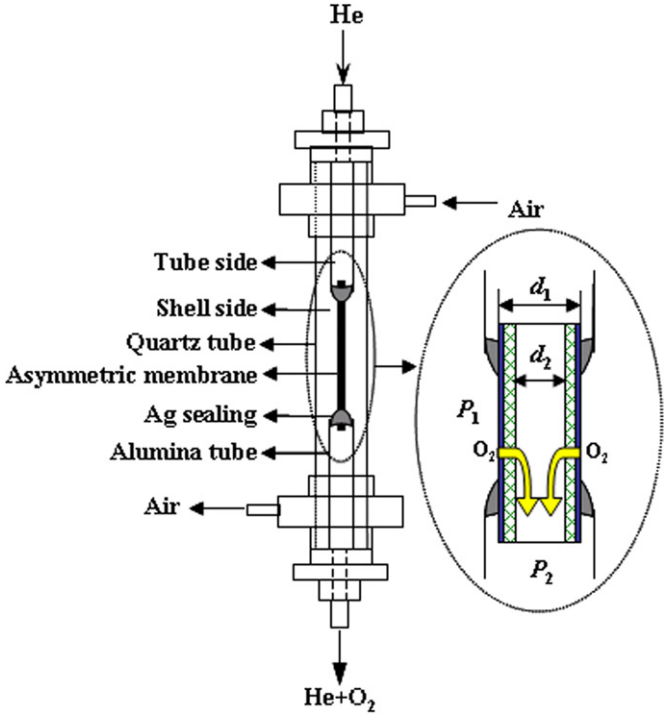

Fig. 3. The module of the high temperature oxygen permeation measurements.

3.2. Sintering behavior of the asymmetric tubular membrane

For the co-sintering method, the match of the sintering behavior between the membrane and support is crucial to obtain a dense and crack-free asymmetric membrane. In other words, during the densification process of the asymmetric membrane, the dimension of the support layer should undergo a similar change to that of the membrane layer. The sintering behavior of a sample can be described by the linear shrinkage rate with increase in temperature and the final shrinkage. Dilatometry is an effective way to measure the sintering behavior of a material in situ, which directly gives the length change of sample (L/L_0) as a function of temperature (T) and time (t). L_0 is the initial length of sample. The sintering behavior of SCFZ membrane layer and support in air is illustrated in Fig. 5. As shown in Fig. 5a, the membrane layer and support undergo different shrinking processes in the tested temperature range. The slight shrinkage before 320 °C is caused by the removal of the pore formers and bound solvent in the samples. The sintering process of membrane layer and support starts at about 740 °C, and the linear shrinkages are 27.9% and 37.7%, respectively at 1250 °C.

To clearly observe the change of a sample length in the sintering process, it may be more useful to give a plot of the sintering rate curve versus the temperature ($dL/dt \sim T$). The sintering rate curve of membrane layer and support is shown in Fig. 5b. During the sintering process (> 700 °C), the sintering rate of the support increases significantly with increase in the temperature, except for some minor fluctuations. In contrast, the sintering rate of the membrane layer increases first, and reaches the maximums at about 920 °C and 1100 °C, finally decreases after 1100 °C. After 1100 °C, the sintering rate of the support is

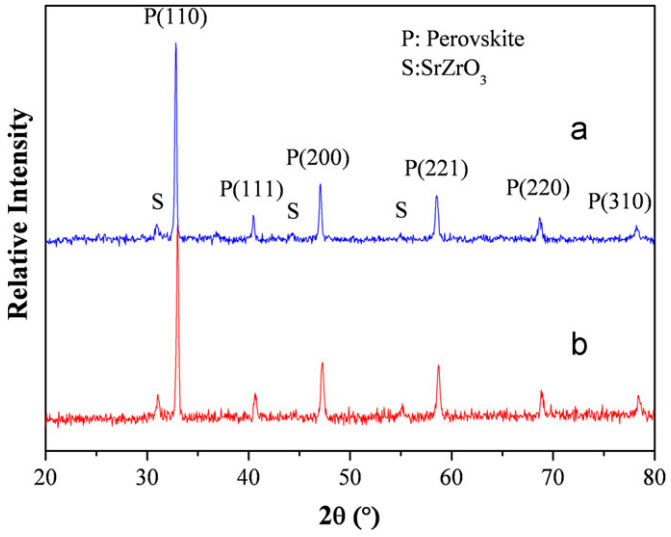

Fig. 4. XRD patterns of the SCFZ powders synthesized by EDTA–citrate complexation method (a) and solid-state reaction method (b).

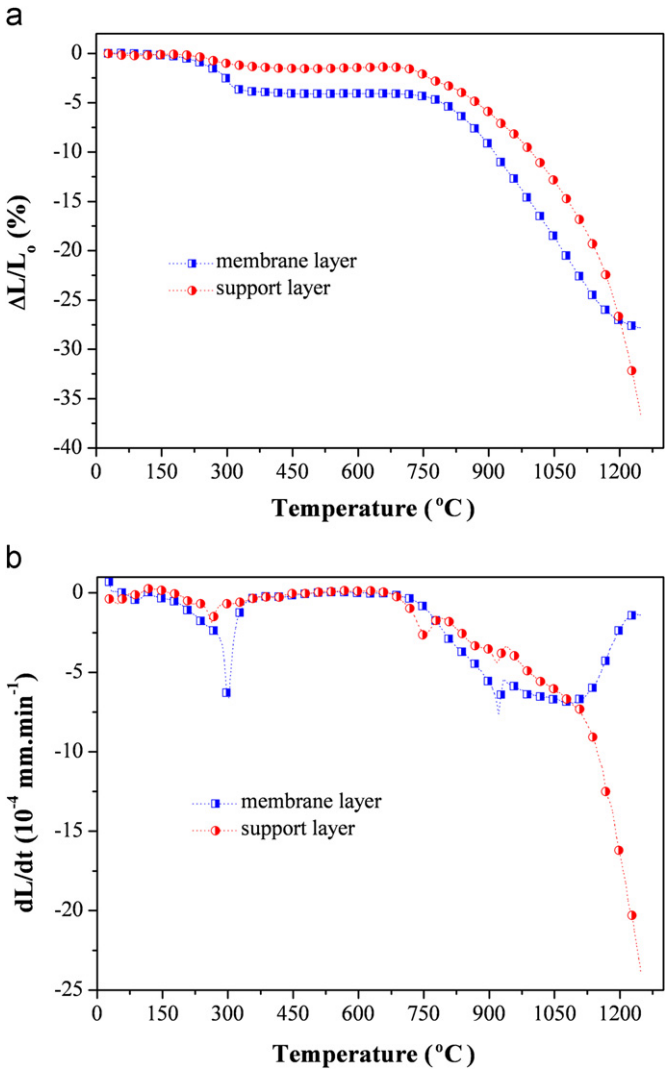

Fig. 5. Dilatometric curves of SCFZ membrane layer and support: (a) shrinkage curves and (b) shrinkage rate.

larger than that of the membrane layer. Therefore, at this sintering stage the shrinkage of membrane is limited by support, which will induce the formation of cracks or defects. In general, the linear shrinkage is a function of multi-factor [25], such as the particle size distribution of ceramic powder, the weight ratio of the ceramic powder to polymer binder and the sintering conditions. In our experiments, to avoid the formation of defects in the membrane, a small heating rate (0.5–1.5 °C min^{-1}) was used at this most important stage. In addition, the ceramic powders with bigger particle size were used for the preparation of support to reduce its sintering rate above 1100 °C.

3.3. Formation of the asymmetric tubular membrane

For separation applications, not only crack-free but also dense asymmetric tubular membranes are required. Therefore, two key factors: spraying circles and sintering temperature were further optimized. As shown in Table 1, dense asymmetric tubular membranes can be prepared at 1250 °C with the spraying circles of 2 or 3. Although the thickness of membrane increases with increase in the spraying circles, the mismatch of the sintering behaviors between the thick membrane layer and the support also increases. Therefore, the spraying circles of 3 were used to ensure that the membranes were dense.

Table 1
Influence of spraying circles and sintering temperature of membrane.

Spraying circles	Sintering temperature (°C)	Macrostructure of membrane	Gas tight
2	1200	Crack-free	No
3	1200	Crack-free	No
4	1200	Crack-free	No
5	1200	Crack-free	No
2	1250	Crack-free	Yes
3	1250	Crack-free	Yes
4	1250	Crack	No
5	1250	Crack	No

Fig. 6 shows the SEM morphology of the tubular asymmetric membrane. From the outside surface of the membrane (Fig. 6a), the ceramic gains with clear grain boundaries are visible, and the membrane surface is dense and free from cracks and holes. A dense membrane layer can be seen in Fig. 6b, and the membrane layer with a thickness of about 20 μm is well bonded with the support. The surface of the support is shown in Fig. 6c. The support is porous and the overall porosity of about 10% was acquired in the tubular body after sintering.

The tightness of membranes was further checked by the N_2 gas-tight test at room temperature. The N_2 with an absolute pressure up to 0.2 MPa was fed into one side of membrane and the permeation of N_2 was not detected at the other side of the membrane. In our oxygen permeation and membrane reaction experiments, the two sides of membrane were both maintained at the atmospheric pressure (0.1 MPa). The pressure difference in the oxygen permeation experiment was less than that in the N_2 gas-tight test, indicating that the asymmetric membrane developed in our work was gas tight enough for the oxygen permeation experiment.

As for the asymmetric membrane structure, the porous support should have low gas transport resistance so that the diffusion of gas in the support does not determine the rate. A green support was sintered under the identical condition with the asymmetric membrane. Fig. 7 shows the nitrogen permeability of the sintered support at room temperature. According to the reports of Lin et al. [26], the average pore size of the support is estimated to be 1.3 μm from Fig. 7, and its nitrogen permeation is controlled by the viscous flow, indicating that the porous support has a low gas transport resistance. There are two paths to simultaneously happen for oxygen to transfer to the support: (i) oxygen molecules transfer through the pore of the support and (ii) oxygen ions transfer through the wall of support. The oxygen ion transfer through the wall of support corresponds to provide a larger surface area for the oxygen surface exchanges on the thin dense layer. If the oxygen flux through the asymmetric membrane is mainly controlled by the surface oxygen exchange, low porosity leads to a smaller surface area for the oxygen surface exchanges, resulting in lower oxygen permeation flux. The porous support can be improved by increasing the mount and size of pore former or making hollow fiber for porous support.

3.4. Oxygen permeability of the asymmetric tubular membrane

The SCFZ asymmetric tubular membrane with the top layer of 20 μm and the porous support of 0.5 mm was applied to evaluate the oxygen permeability. For comparison, the oxygen permeation flux of the SCFZ tubular membrane (i.d.=1.5 mm, o.d.=2.5 mm) was tested. The temperature dependence of oxygen flux through the asymmetric and symmetric membranes is shown in Fig. 8. All the samples were measured at identical experimental conditions.

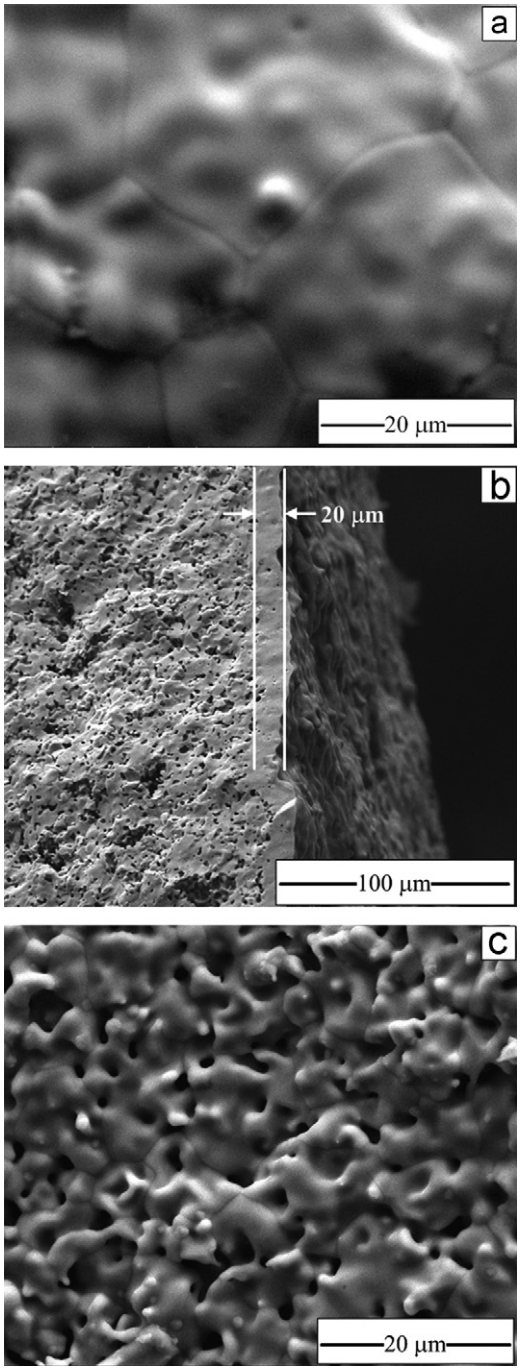

Fig. 6. SEM image of SCFZ tubular asymmetric membrane: (a) outside surface, (b) cross section and (c) inside surface.

The oxygen permeabilities of the symmetric and asymmetric membranes were measured in the temperature range 800–900 °C. The oxygen permeation flux increases sharply with increase in the temperature, which mainly attributed to the promotion of the oxygen diffusion and the oxygen surface reaction rates. The oxygen permeation flux of the asymmetric membrane is higher than that of the symmetric tubular membrane. At 800 °C, the oxygen permeation flux of the asymmetric membrane is 7.41×10^{-7} mol cm^{-2} s^{-1}, which is 2.35 times that of the sintered SCFZ tubular membrane, 3.15×10^{-7} mol cm^{-2} s^{-1}. At 900 °C, the oxygen permeation flux reached 1.37×10^{-6} mol cm^{-2} s^{-1}. To obtain accurate Arrhenius activation energies (Ea) for oxygen transport through membranes, the oxygen partial pressure gradient was fixed at 21 kPa/0.3 kPa by

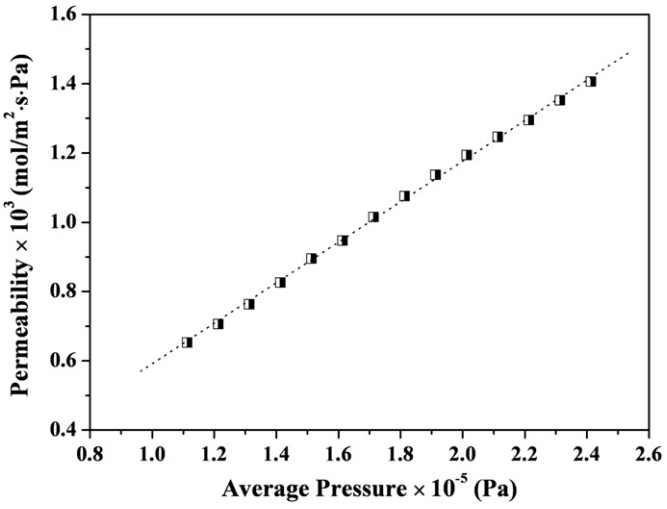

Fig. 7. Nitrogen permeability of the support at room temperature.

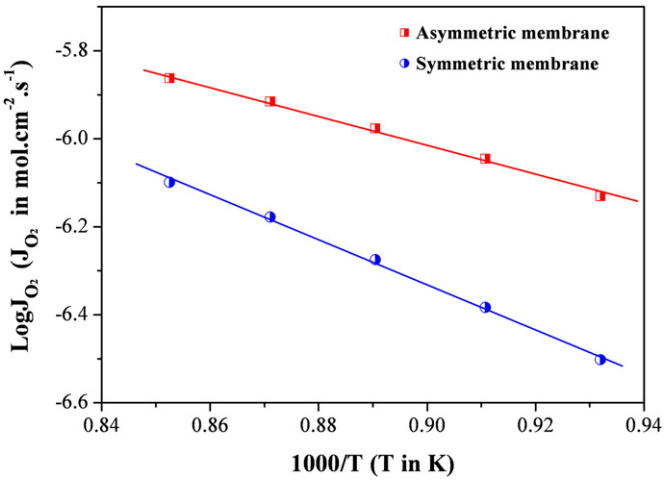

Fig. 8. Arrhenius plots of the oxygen fluxes of the asymmetric tubular membrane, and sintered symmetric SCFZ tubular membrane.

adjusting the helium flow rate during the change of temperature. From Fig. 8, the apparent activation energies of the asymmetric tubular membrane and SCFZ tubular membrane are estimated to be 64.4 kJ/mol and 97.6 kJ/mol in the temperature range 800–900 °C, respectively, indicating the asymmetric membrane has a greater capability for the oxygen permeation than the symmetric membrane. Similar results were observed by Teraoka et al. [9] for the $La_{0.6}Sr_{0.4}CoO_{3-\delta}$ supported membrane and Jin et al. [13] for the $La_{0.6}Sr_{0.4}Co_{0.2}Fe_{0.8}O_{3-\delta}$ supported membrane.

For the mixed-conducting membrane, the overall oxygen permeation process is generally divided into the surface reactions on the two sides of the membrane and the bulk diffusion through the membrane [1]. For the membrane thickness less than the characteristic thickness (L_c), the oxygen permeation flux through the membrane is controlled by the surface oxygen exchange reactions on both sides of the membrane, and is not sensitive to the membrane thickness. In our previous work [27], the L_c of the SCFZ membrane was estimated to be ~59 μm. In this work, the dense membrane layer is 20 μm, which is smaller than the L_c. The oxygen flux through the membrane is therefore controlled by the surface oxygen exchange process.

Based on the assumptions discussed by Kim et al. [28], if the oxygen permeation process is limited by the rate of oxygen exchange on the membrane surface, the oxygen permeation flux

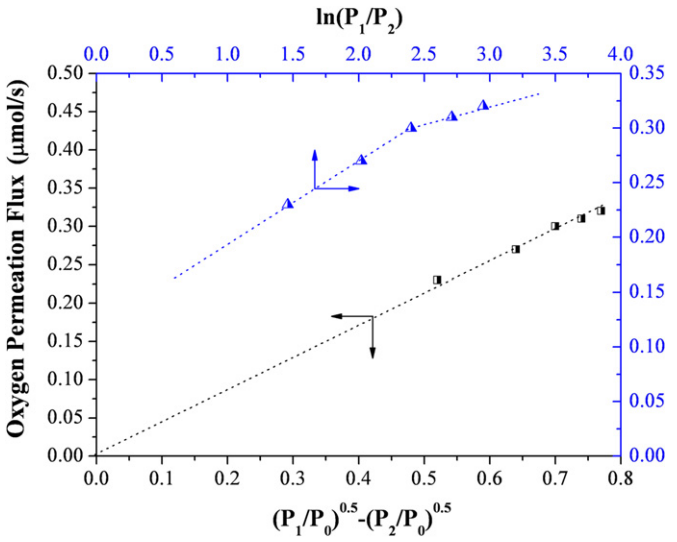

Fig. 9. Oxygen flux of the asymmetric tubular membrane against $(P_1/P_0)^{0.5}-(P_2/P_0)^{0.5}$ and $\ln(P_1/P_0)$ at 850 °C. Conditions: $P_1=1$ atm; P_2 varied from 0.01 to 0.05 atm; $d_1=0.22$ cm; $d_2=0.12$ cm; $w=0.54$ cm.

will be linearly proportion to the pressure term $(P_1/P_0)^{0.5}-(P_2/P_0)^{0.5}$, the following relation should be hold:

$$J_{O_2}=\frac{\pi d_1 d_2 w c_i k_{io}}{d_1+d_2}\left(\sqrt{P_1/P_0}-\sqrt{P_2/P_0}\right) \quad (2)$$

where k_{io} (cm/s) is surface exchange coefficient; c_i (mol/cm^3) the density of oxygen ions. P (atm) is the gas pressure and the subscript 0, 1, 2 indicate 1 atm of oxygen pressure, the oxygen partial pressure on the shell side and on the tube side, respectively.

On the other hand, when the oxygen permeation process is mainly controlled by the bulk diffusion, the oxygen permeation flux, is linearly proportional to $\ln(P_1/P_2)$, the oxygen permeation flux can be expressed as

$$J_{O_2}=\frac{\pi w c_i D_a}{2\ln(d_1/d_2)}\ln(P_1/P_2) \quad (3)$$

where D_a is the ambipolar oxygen ion–electron hole bulk diffusion coefficient. Fig. 9 plots the oxygen permeation flux against the oxygen partial pressure terms according to Eqs. (2) and (3) at 850 °C. A linear relationship between oxygen permeation flux and $(P_1/P_0)^{0.5}-(P_2/P_0)^{0.5}$ can be observed. The surface exchange coefficient is estimated to be 3.04×10^{-6} cm s^{-1}. Meanwhile, a no linear relationship between oxygen permeation flux and $\ln(P_1/P_0)$ was found, indicating the oxygen transport is mainly controlled by surface exchange.

For the practical application, the asymmetric membrane must exhibit the long-term stability at the elevated temperature and the low oxygen partial pressure. Fig. 10 shows the stability of the oxygen permeation of asymmetric membrane at the temperature of 850 °C. It can be seen that the oxygen flux maintains at about 1.06×10^{-6} mol cm^{-2} s^{-1} during the testing period. After the oxygen permeation measurement of the supported membrane lasted for 200 h, the experiment was voluntarily stopped, and no cracks were found in the membrane, indicating the supported dense membrane was stable under low oxygen partial pressure.

4. Conclusions

Our study demonstrates that a continuous crack-free asymmetric tubular membrane can be successfully prepared by a combined spin-spraying and co-sintering method, which is a simple and cost-effective manufacturing process. The optimization of prepared condition such as sintering temperature, heating rate and spraying circles, led to formation of asymmetric membranes with desired structure. A sintering temperature of 1250 °C proved to be the optimum final sintering temperature. The thickness of the membrane prepared using the three times spraying circle is 20 μm. The asymmetric tubular membrane exhibited the high oxygen permeation rate which is 135% higher than that of the symmetric membrane at 800 °C, and stable oxygen permeation about 200 h at low oxygen partial pressure atmosphere. The oxygen transport is mainly controlled by surface exchange, and the surface exchange coefficient is estimated to be 3.04×10^{-6} cm s^{-1} at 850 °C.

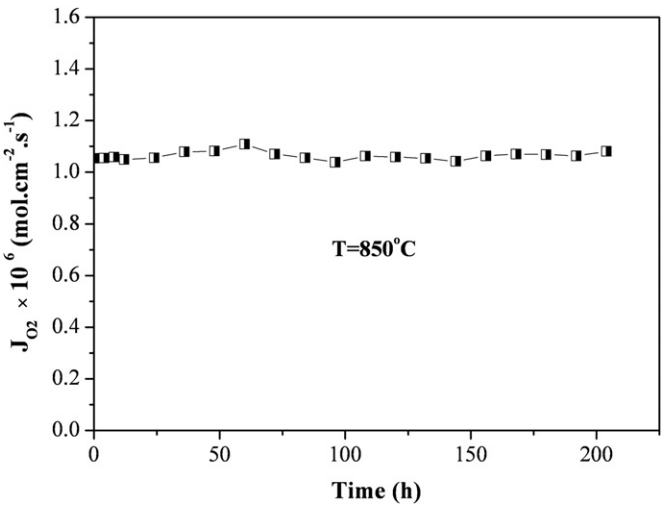

Fig. 10. Time dependence of the oxygen permeation fluxes through the asymmetric membrane at 850 °C.

Nomenclature

List of symbols

c_i	density of oxygen ions (mol cm^{-3})
D_a	bulk diffusion coefficient (cm^2 s^{-1})
d_1	outside diameter of the tube (cm)
d_2	inside diameter of the tube (cm)
F	Faraday constant (C/mol)
J_{O_2}	oxygen permeation flux (mol cm^{-2} s^{-1})
k_{io}	Surface exchange coefficient (cm s^{-1})
L	membrane thickness (cm)
L_c	characteristic membrane thickness (cm)
P_{O_2}	oxygen partial pressure (Pa)
Q	flow rate of the sweep stream (ml/min)
R	gas constant (J/mol K)
S	membrane area (cm^2)
w	length of the tube (cm)

Greek symbols

σ_i	ionic conductivities (S/m)
σ_e	electronic conductivities (S/m)

Acknowledgments

This work was supported by the National Basic Research Program of China (No. 2009CB623406), National Natural Science

Foundation of China (No. 20990222, 21006047), and A Project Funded by the Priority Academic Program Development of Jiangsu Higher Education Institutions.

References

[1] H.J.M. Bouwmeester, A.J. Burggraaf, Dense ceramic membranes for oxygen separation, in: A.J. Burggraaf, L. Cot (Eds.), Fundamentals of Inorganic Membrane Science Technology, Elsevier, Amsterdam, 1996. 435–515.
[2] E.V. Tsipis, V.V. Kharton, Electrode materials and reaction mechanisms in solid oxide fuel cells: a brief review, J. Solid State Electrochem. 12 (2008) 1367.
[3] A.J. Jacobson, Materials for solid oxide fuel cells, Chem. Mater. 22 (2010) 660.
[4] X.L. Dong, W.Q. Jin, N.P. Xu, K. Li, Dense ceramic catalytic membrane and membrane reactors for energy and environment applications, Chem. Commun. 47 (2011) 10886.
[5] J. Sunarso, S. Baumann, J.M. Serrac, W.A. Meulenbergb, S. Liua, Y.S. Lin, J.C. Diniz da Costa, Mixed ionic–electronic conducting (MIEC) ceramic-based membranes for oxygen separation, J. Membr. Sci. 320 (2008) 13.
[6] X.Y. Tan, K. Li, Design of mixed conducting ceramic membranes/reactors for the partial oxidation of methane to syngas, AICHE J. 55 (2009) 2675.
[7] H. Jiang, H. Wang, S. Werth, T. Schiestel, J. Caro, Simultaneous production of hydrogen and synthesis gas by combining water splitting with partial oxidation of methane in a hollow-fiber membrane reactor, Angew. Chem. Int. Ed. 47 (2008) 9341.
[8] X.Y. Tan, K. Li, A. Thursfield, I.S. Metcalfe, Oxyfuel combustion using a catalytic ceramic membrane reactor, Catal. Today 131 (2008) 292.
[9] Y. Teraoka, T. Fukuda, N. Miura, N. Yamazoe, Development of oxygen semipermeable membrane using mixed conductive perovskite-type oxides (Part 2), J. Ceram. Soc. Jpn. Int. Ed. 97 (1989) 523.
[10] H.X. Luo, K. Efimov, H.Q. Jiang, A. Feldhoff, H.H. Wang, J. Caro, CO(2)-Stable and cobalt-free dual-phase membrane for oxygen separation, Angew. Chem. Int. Ed. 50 (2011) 759.
[11] X.F. Zhu, Q.M. Li, Y.Y. He, Y. Cong, W.S. Yang, Oxygen permeation and partial oxidation of methane in dual-phase membrane reactors, J. Membr. Sci. 360 (2010) 454.
[12] C. Wagner, Equations for transport in solid oxides and sulfides of transition metals, Prog. Solid State Chem. 10 (1975) 3–16.
[13] W.Q. Jin, S.G. Li, P. Huang, N.P. Xu, J. Shi, Preparation of an asymmetric perovskite-type membrane and its oxygen permeability, J. Membr. Sci. 185 (2001) 237.
[14] A. Kawahara, Y. Takahashi, Y. Hirano, M. Hirano, T. Ishihara., High oxygen permeation rate in $La_{0.6}Sr_{0.4}Ti_{0.3}Fe_{0.7}O_3$ thin membrane on a porous support with multichannel structure for CH_4 partial oxidation, Ind. Eng. Chem. Res. 49 (2010) 5511.
[15] X.L. Dong, C. Zhang, X.F. Chang, W.Q. Jin, N.P. Xu, A self-catalytic membrane reactor based on a supported mixed-conducting membrane, AIChE J. 54 (2008) 1678.
[16] S. Araki, Y. Hoshi, S. Hamakawa, S. Hikazudani, F. Mizukami, Synthesis and characterization of mixed ionic-electronic conducting $Ca_{0.8}Sr_{0.2}Ti_{0.7}Fe_{0.3}O_{3-a}$ thin film, Solid State Ionics 178 (2008) 1740.
[17] A. Julian, E. Juste, P.M. Geffroy, V. Coudert, S. Degot, P. Del Gallo, N. Richet, T. Chartier, Elaboration of $La_{0.8}Sr_{0.2}Fe_{0.7}Ga_{0.3}O_{3-delta}/La_{0.8}M_{0.2}Fe_{O3-\delta}$ (M=Ca, Sr and Ba) asymmetric membranes by tape-casting and co-firing, J. Membr. Sci. 333 (2009) 132.
[18] K. Watanabe, M. Yuasa, T. Kida, K. Shimanoe, Y. Teraoka, N. Yamazoe, Dense/porous asymmetric-structured oxygen permeable membranes based on $La_{0.6}Ca_{0.4}CoO_3$ perovskite-type oxide, Chem. Mater 20 (2008) 6965.
[19] A.V. Kovalevsky, V.V. Kharton, F.M.M. Snijkers, J.F.C. Cooymans, J.J. Luyten, J.R. Frade, Processing and oxygen permeability of asymmetric ferrite-based ceramic membranes, Solid State Ionics 178 (2008) 64.
[20] X.F. Chang, C. Zhang, W.Q. Jin, N.P. Xu, Match of thermal performances between the membrane and the support for supported dense mixed-conducting membranes, J. Membr. Sci. 285 (2006) 232.
[21] X. Yin, L. Hong, Z.L. Liu, Oxygen permeation through the LSCO-80/CeO_2 asymmetric tubular membrane reactor, J. Membr. Sci. 268 (2006) 2.
[22] W. Ito, T. Nagai, T. Sakon, Oxygen separation from compressed air using a mixed conducting perovskite-type oxide membrane, Solid State Ionics 178 (2007) 809.
[23] M.B. Choi, S.J. Song, T.W. Lee, H.I. Yoo, U.D. Lee, B.R. Bang, Preparation of asymmetric tubular oxygen separation membrane with oxygen permeable $Pr_2Ni_{0.75}Cu_{0.25}Ga_{0.05}O_{4+\delta}$, Int. J. Appl. Ceram. Technol. 8 (2011) 800.
[24] M. Ikeguchi, K. Ishii, Y. Sekine, E. Kikuchi, M. Matsukata, Improving oxygen permeability in $SrFeCo_{0.5}O_x$ asymmetric membranes by modifying support-layer porous structure, Mater. Lett. 59 (2005) 1356.
[25] S.M. Liu, G.R. Gavas, Perparation of oxygen ion conducting ceramic hollow-fiber membranes, Ind. Eng. Chem. Res. 44 (2005) 7633.
[26] Y.S. Lin, A.J. Burggraaf, Experimental studies on pore size change of porous ceramic membranes after modification, J. Membr. Sci. 79 (1993) 65.
[27] X.F. Chang, C. Zhang, Z.T. Wu, W.Q. Jin, N.P. Xu, Contribution of the surface reactions to the overall oxygen permeation of the mixed conducting membranes, Ind. Eng. Chem. Res. 45 (2006) 2824.
[28] S. Kim, Y.L. Yang, A.J. Jacobson, B. Abeles, Diffusion and surface exchange coefficients in mixed ionic electronic conducting oxides from the pressure dependence of oxygen permeation, Solid State Ionics 106 (1998) 189.